Superconductivity in spinel-type compounds CuRh2S4 and CuRh2Se4

Superconductivity in spinel-type compounds $CuRh_2S_4$ and $CuRh_2Se_4$

Takatsugu Hagino and Yoshitaka Seki
Department of Materials Science and Engineering, Muroran Institute of Technology, Mizumoto-cho 27-1, Muroran 050, Japan

Nobuo Wada
Department of Physics, College of Arts and Science, University of Tokyo, Tokyo 153, Japan

Seigo Tsuji
Department of Physics, Faculty of Science, Hokkaido University, Sapporo 060, Japan

Takashi Shirane
Department of Materials Science and Engineering, Muroran Institute of Technology, Mizumoto-cho 27-1, Muroran 050, Japan

Ken-ichi Kumagai
Department of Physics, Faculty of Science, Hokkaido University, Sapporo 060, Japan

Shoichi Nagata*
Department of Materials Science and Engineering, Muroran Institute of Technology, Mizumoto-cho 27-1, Muroran 050, Japan
(Received 18 November 1994)

An extensive study of electrical resistivity, ac magnetic susceptibility, magnetization, specific heat, and NMR has been made on high purity samples of the spinel compounds $CuRh_2S_4$ and $CuRh_2Se_4$. The superconducting transitions occur at 4.70 K in $CuRh_2S_4$ and 3.48 K in $CuRh_2Se_4$. The magnetic susceptibilities show perfect diamagnetism in both compounds. Upper critical fields at $T=0$ are estimated to be 20.0 and 4.40 kOe, the lower critical fields at $T=0$ are 70 and 95 Oe, respectively. The thermodynamic critical fields at $T=0$ are 704 Oe ($CuRh_2S_4$) and 445 Oe ($CuRh_2Se_4$). These values are obtained from the temperature dependence of the free energy. These compounds are type-II superconductors with Ginzburg-Landau parameters $\kappa=21$ ($CuRh_2S_4$) and $\kappa=6.6$ ($CuRh_2Se_4$) at $T=0$. The electron-phonon coupling constants, $\lambda_{ep}=0.68$ ($CuRh_2S_4$) and $\lambda_{ep}=0.64$ ($CuRh_2Se_4$), are obtained using the McMillan formula. The copper nuclear-spin-relaxation rate as a function of temperature shows a pronounced coherence peak just below T_c for $CuRh_2S_4$. Experimental results are analyzed on the basis of the BCS theory. These compounds exist between weak- and intermediate-coupling superconductors which are driven by electron-phonon interaction. The Debye temperatures Θ of these materials are 230 K ($CuRh_2S_4$) and 211 K ($CuRh_2Se_4$).

I. INTRODUCTION

The ternary sulpho- and selenospinels $CuRh_2S_4$ and $CuRh_2Se_4$ have the cubic spinel structure (Fig. 1) at room temperature and have lattice constants of $a=9.787$ and 10.269 Å, respectively. They have the normal spinel structure where the Cu ions occupy the A (tetrahedral) sites and the Rh ions occupy the B (octahedral) sites. The trivalent Rh ions at B sites are in the low-spin state ($4d^6$:t_{2g}^6,e_g^0) with no magnetic moment in a strong crystalline field. The valence of Cu has been the subject of controversy.[1,2]

The ternary sulpho- and selenospinels $CuRh_2S_4$ and $CuRh_2Se_4$ show metallic conduction and nearly temperature-independent susceptibility. The electrical and magnetic properties of these compounds at high temperatures have been discussed by Lotgering and Van Stapele.[3]

On the other hand, it has been reported that these compounds $CuRh_2S_4$ and $CuRh_2Se_4$ reveal superconducting transitions between 3 and 4 K. Only brief reports have been given by earlier workers,[4–11] and no detailed study and analysis associated with the superconductivity have been made so far to our knowledge.

In this paper, we report experiments designed to explore in greater detail the superconducting characteristics of these spinel compounds. In order to elucidate these characteristics with an emphasis on the low-temperature region, we have carried out the following measurements: the temperature dependences of (1) electrical resistivity ρ, (2) diamagnetic ac and dc susceptibilities χ, (3) magnetization M, (4) specific heat, and (5) copper NMR. These experimental results are discussed in terms of the BCS theory.

In addition, the normal-state electrical, magnetic, and thermal properties are also examined. In particular, the electrical resistivities of these materials in the normal state have similar characteristics to A-15 compounds such as Nb_3Sn.

0163-1829/95/51(18)/12673(12)/$06.00

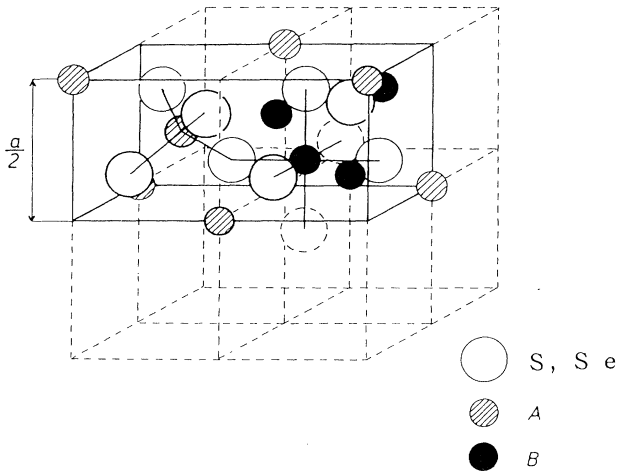

FIG. 1. The cubic unit cell of the spinel structure with lattice parameter a. Shaded circles A (Cu ions) lie on the corner and in the center of an octant. Black circles B (Rh ions) and white circles (S or Se ions) lie on the body diagonals of the octants at $\frac{1}{4}$ of their lengths.

II. EXPERIMENTAL METHODS

A. Sample preparation

Mixtures of high-purity fine powders of Cu, Rh, S, or Se with nominal stoichiometry were heated in sealed quartz tubes at 850 °C for periods of 10 days. Subsequently, the specimens were reground and sintered in pressed parallelepiped form at 850 °C for 48 h. X-ray diffraction data confirm the spinel phase in these powder specimens. Samples with dimensions of about $2.0\times2.0\times10$ mm^3 were used for the measurements of ρ and ac susceptibility χ. For the magnetization (M-H curves), the sample dimensions were $1.0\times1.0\times8.0$ mm^3 with the fields applied parallel to the longest dimension. The filling densities of a sintered bar sample are 70% ($CuRh_2S_4$) and 87% ($CuRh_2Se_4$) in comparison with the values of single crystals (theoretical density).

B. Electrical resistivity measurements

The temperature dependence of the electrical resistivity was measured over the temperature region between 1.5 and 285 K. The resistivity was measured by a standard four-probe method. Silver paste was used to fabricate the electrodes.

C. ac magnetic susceptibility measurements

ac complex magnetic susceptibility, $\chi=\chi'-i\chi''$, was measured by using a Hartshörn bridge and a two-phase lock-in amplifier in the temperature range between 1.6 and 285 K. The operating frequency was 80 Hz and the amplitude of the ac magnetic field was 1.0 Oe. A parallelepiped-shaped sample was used with the longest dimension parallel to the magnetic field. Demagnetizing-field corrections were made for the sample, assuming completely homogeneous sintering in the whole specimen. The magnitude of the corrections in χ was evaluated to be less than 12%.

D. Specific-heat measurements

The specific-heat measurements were done using a conventional ^{3}He cryostat. For specific heat, a standard heat-pulse technique was employed. The addenda included the thermometer, heater, glue, etc. The corrections due to the addenda were made. The specific-heat measurements were performed in the temperature ranges between 1.69 and 16.3 K for $CuRh_2S_4$ and 0.60 and 15.2 K for $CuRh_2Se_4$. Several sintered samples with total masses of 0.828 g ($CuRh_2S_4$) and 1.262 g ($CuRh_2Se_4$) were used for these measurements.

E. dc magnetization

The dc magnetization curves at constant temperatures and the temperature dependences of the magnetization at a constant applied magnetic field of 10 kOe were performed with a Quantum Design superconducting quantum interference device (SQUID). The values of upper critical field H_{c2} were obtained by the magnetization curves up to only 10 kOe because of the limits of our apparatus.

F. Cu NMR in $CuRh_2S_4$

A conventional phase-coherent pulsed NMR apparatus was used for measurements of the spectra of Cu nuclei and the nuclear spin-lattice relaxation time T_1.[12,13] The samples were crushed into a fine powder for these measurements. The copper NMR spectrum was obtained by (a) sweeping the magnetic field while maintaining a constant frequency of 12.5 MHz and (b) maintaining a constant field of 11 kOe. The Knight shift was determined by the gyromagnetic ratio for ^{63}Cu and the reference value of metallic Cu. The T_1 measurements were made down to 1.4 K. Detailed NMR experimental results will be published elsewhere.[14]

III. RESULTS AND DISCUSSION

A. X-ray powder diffraction

Figures 2 and 3 present the x-ray diffraction patterns at room temperature for the samples $CuRh_2S_4$ and $CuRh_2Se_4$. As can be seen in Figs. 2 and 3, all the diffraction peaks have been indexed to the cubic unit cell. These indexed peaks have (h,k,l) values that are either all even or all odd, which is consistent with a fcc unit cell. Both samples are single phase.

B. Electrical resistivity

Figures 4 and 5 show the resistivity as a function of temperature. With decreasing temperature, the resistivities ρ decrease monotonically with shallow upturned curvatures and abrupt superconducting transitions at 4.70

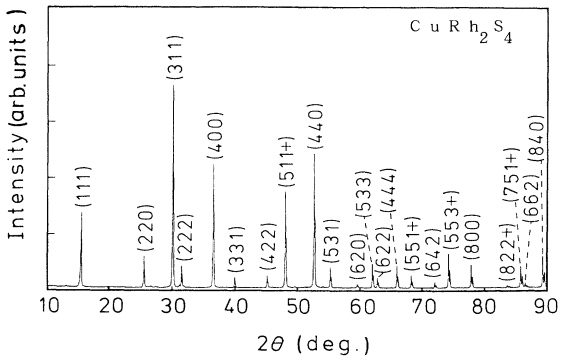

FIG. 2. X-ray diffraction pattern of $CuRh_2S_4$ with peaks indexed to $a = 9.787$ Å.

and 3.48 K (midpoints) for the samples $CuRh_2S_4$ and $CuRh_2Se_4$, respectively.

In $CuRh_2S_4$, the resistivity was measured with a current density of 0.47A/cm^2. The resistivity at 300 K is about $8\times10^{-3}\Omega$ cm and the residual value of ρ_0 is estimated to be $4.1\times10^{-4}\Omega$ cm in the sintered specimen.

In the $CuRh_2Se_4$ sample, the resistivity at 300 K is about $4.6\times10^{-4}\Omega$ cm and just above T_c the resistivity ρ_0 is about $2.3\times10^{-6}\Omega$ cm. The data for $CuRh_2Se_4$ are scattered at low temperatures because the resistivity becomes extremely small. Because of this low resistivity, a current density of 2.63 A/cm^2 was used. It should be noted that such a high current density might suppress T_c slightly.

$CuRh_2S_4$ has a 17 times larger resistivity than $CuRh_2Se_4$. The sample filling density is larger for $CuRh_2Se_4$ than that of $CuRh_2S_4$. Furthermore, in the $CuRh_2Se_4$ sample, the selenium anion has a larger ionic radius than that of sulfur and thus overlappings of the wave function between anions and cations are larger. Consequently, stronger covalent bonds and lower resistivity are expected for $CuRh_2Se_4$.

In the low-temperature range from T_c to 20 K, the $\rho(T)$ of $CuRh_2S_4$ and $CuRh_2Se_4$ can be expressed well as a power law:

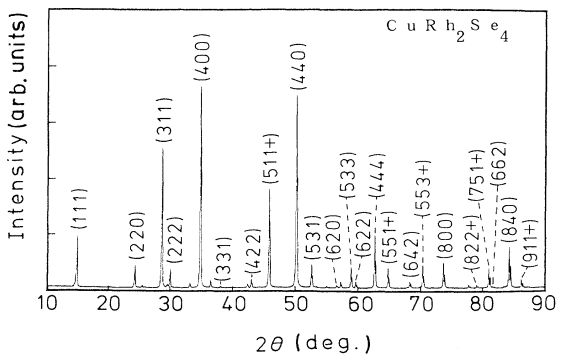

FIG. 3. X-ray diffraction pattern of $CuRh_2Se_4$ with peaks indexed to $a = 10.269$ Å.

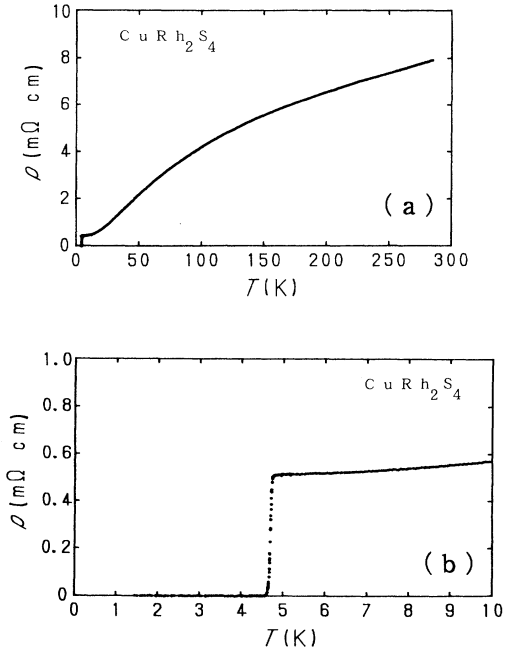

FIG. 4. (a) Temperature dependence of the resistivity of a sintered sample $CuRh_2S_4$ over a temperature range of 4.2 to 285 K. (b) Temperature dependence of the resistivity between 1.5 and 10 K.

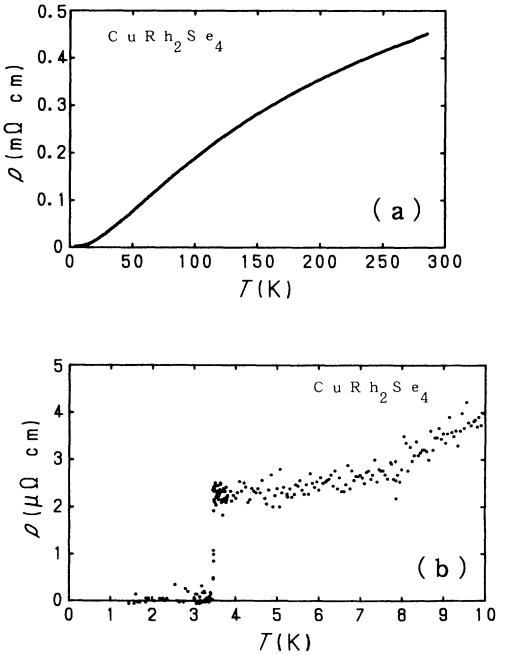

FIG. 5. (a) Temperature dependence of the resistivity of a sintered sample $CuRh_2Se_4$ over a temperature range of 4.2 to 285 K. (b) Temperature dependence of the resistivity between 1.5 and 10 K.

$$\rho(T)=\rho_0+AT^n\ , \tag{1}$$

where A and n are constants. From the slope of the straight line in plots of $\log_{10}[\rho(T)-\rho_0]$ vs $\log_{10}T$ (Figs. 6 and 7), the value of n has been determined to be 3.1 and 2.8 for $CuRh_2S_4$ and $CuRh_2Se_4$. The temperature dependence of $\rho(T)$ becomes weaker above 20 K. At high temperatures, $\rho(T)$ tends to a linear function of T. The same behavior of the normal-state resistivity has been reported in the superconductor $Th_3Ni_3Sn_4$.[15] The power law and the values of n close to 3.0 suggest that there exists a state density of d electrons at the Fermi energy, which is consistent with the spin fluctuation expected from the enhanced susceptibility. A T^3 dependence follows from the Wilson s-d scattering model.[16]

While carrying out the resistivity measurements over a wider temperature range, we also noticed that the temperature dependence of $\rho(T)$ appears to be similar to that of A-15 materials. It should be noted that in A-15 structure intermetallic compounds, such as Nb_3Sn and Nb_3Al, the resistivity can be fitted to the simple form expressed as[17]

$$\rho(T)=\rho_0+\rho_1T+\rho_2\exp[-T_0/T]\ , \tag{2}$$

where ρ_0, ρ_1, ρ_2, and T_0 are constants independent of temperature T. Several mechanisms have been presented that lead to departures from the temperature dependence predicted by the simple theory of metals. Several theoretical models were considered in order to explain Eq. (2) but none was found to be satisfactory.[17] If one considers the possibility of scattering into the high-density band from the low-mass band, there is an additional contribution to the resistivity. Wilson has accounted for the fact that at high temperatures the resistivity is linear in T and at low temperatures there is an exponential dropoff, reflecting the absence of high-temperature phonons.[18]

Our experimental results of the resistivity of $CuRh_2S_4$ and $CuRh_2Se_4$ can also be described by Eq. (2) over the entire temperature ranges $T_c<T<300$ K. We obtain $\rho_0=4.10\times10^{-4}$ Ω cm, $\rho_1=9.24\times10^{-6}$ Ω cm/K, $\rho_2=6.45\times10^{-6}$ Ω cm, and $T_0=81.49$ K for $CuRh_2S_4$; $\rho_0=2.30\times10^{-6}$ Ω cm, $\rho_1=6.81\times10^{-7}$ Ω cm/K, $\rho_2=3.84\times10^{-4}$ Ω cm, and $T_0=115.6$ K for $CuRh_2Se_4$. These resistivity coefficients are obtained by use of the least-squares fitting method. Our data indicate that the values of ρ_0, ρ_1, and ρ_2 are much larger than those of A-15 materials because of the sintered samples for our measurements, while the values of T_0 give the inherent values of these compounds.

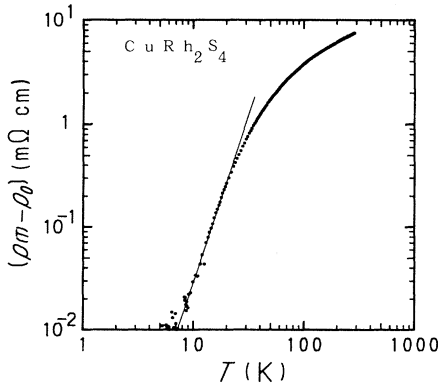

FIG. 6. $\mathrm{Log}_{10}[\rho(T)-\rho_0]$ vs $\log_{10}T$ plot for $CuRh_2S_4$. The straight line is a fit of Eq. (1) to the data points using $n=3.1$.

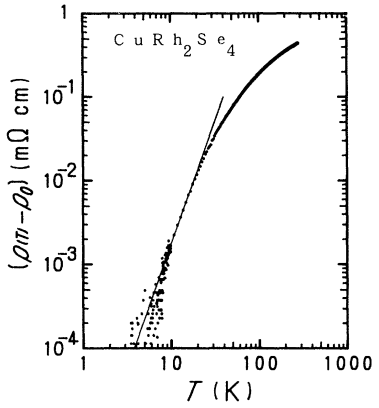

FIG. 7. $\log_{10}[\rho(T)-\rho_0]$ vs $\log_{10}T$ plot for $CuRh_2Se_4$. The straight line is a fit of Eq. (1) to the data points using $n=2.8$.

C. ac magnetic susceptibility and dc magnetic susceptibility

Figures 8 and 9 show the real part of the ac-magnetic susceptibility, χ', as a function of temperature for the sintered bulk samples of $CuRh_2S_4$ and $CuRh_2Se_4$. The superconducting transitions are rather sharp as was observed in the resistivity data. This indicates high homogeneity of the samples. The magnitude of the diamagnetic susceptibilities indicates almost perfect diamagnetism after the demagnetizing-field corrections.

The demagnetizing-field corrections have been made as follows. The bulk susceptibility χ was measured on a sintered sample with the form of a long rod with the applied magnetic field parallel to the long axis of the rod. We then use the following formulas:[19]

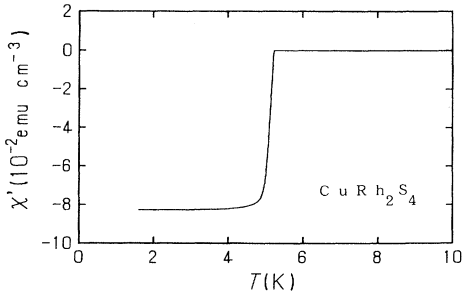

FIG. 8. Real part of the ac magnetic susceptibility as a function of temperature ($1.6<T<10$ K) for the sintered bulk sample $CuRh_2S_4$.

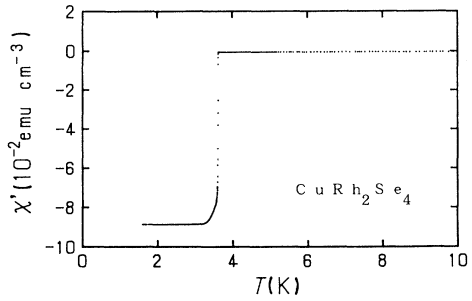

FIG. 9. Real part of the ac magnetic susceptibility as a function of temperature ($1.6 < T < 10$ K) for the sintered bulk sample $CuRh_2Se_4$.

$$\chi = \frac{\chi_a}{1+N\chi_a} , \tag{3}$$

$$N = \frac{4\pi}{2(2m/\sqrt{\pi})+1} \quad \text{(in cgs units)} , \tag{4}$$

$$m = 3.893 \quad (CuRh_2S_4) ,$$

$$m = 3.647 \quad (CuRh_2Se_4) .$$

Here, χ_a is defined as $M = \chi_a H_a$, where H_a is the applied field and M is the magnetization. The form of the demagnetization factor N in Eq. (3) is based on the theory of Sato and Ishii.[19] An approximate expression for the demagnetizing factor for a rectangular plate is used, where m is the dimensional ratio of the sample (see Ref. 19).

The imaginary parts of the ac magnetic susceptibilities, χ'', exhibit sharp maxima at the temperatures of the inflection in χ'. The transition temperatures in the susceptibilities are higher than those observed in the resistivity and the specific heat. The errors of temperature measurements in the ac susceptibilities presumably come from poor thermal contact between the sample and the thermometer.

dc magnetic susceptibilities, which refer to the magnetization M divided by a constant applied field of 10 kOe, M/H, were measured with the SQUID and are presented in Fig. 10. These results of the susceptibility are in fairly good agreement with those of former workers.[3] The gaps in data near 50 K indicate no good result. The experimental results showed a small and broad peak around 50 K associated with the paramagnetic-antiferromagnetic transition of a condensed film of oxygen[20] in the SQUID sample chamber, thus we omitted the unreliable data. At the lowest temperatures, M/H increased rapidly; this may arise from a small Curie contribution due to paramagnetic impurities. The data cannot be well fitted to any reasonable form over a wide temperature range. As a simple assumption, if we take the values of the temperature-independent molar susceptibilities, χ_0, at 300 K, the magnitudes of χ_0 are obtained as $\chi_0(CuRh_2S_4) \sim 1.51\times10^{-4}$ and $\chi_0(CuRh_2Se_4) \sim 9.9\times10^{-5}$ emu/mol f.u. These susceptibilities include a diamagnetic term, χ_{core}, which has been evaluated to be -6.3×10^{-5} emu/mol f.u. for the similar normal-spinel compound $CuIr_2S_4$.[21–24] The susceptibility χ_{core} is the orbital diamagnetism contribution due to ion cores and the value is well within reasonable limits.[25]

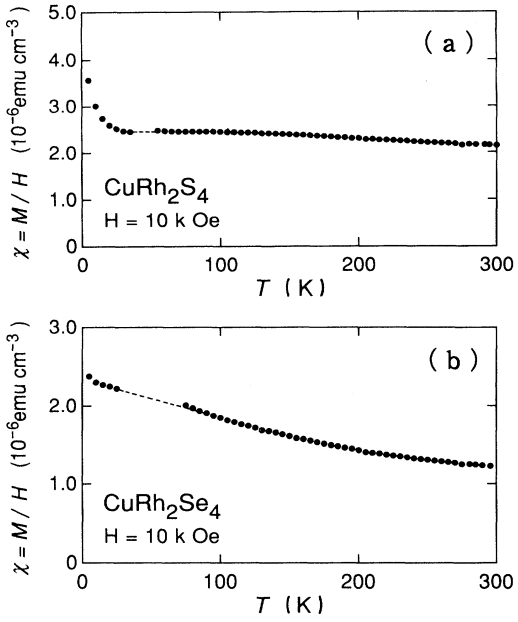

FIG. 10. (a) dc magnetic susceptibility as a function of temperature for $CuRh_2S_4$, where M is the dc magnetization measured with the SQUID. (b) dc magnetic susceptibility of $CuRh_2Se_4$. The gaps in data near 50 K indicate no good result due to an oxygen contamination problem (see text).

After the correction for the diamagnetic contribution, we can estimate the density of states at the Fermi energy $N(\varepsilon_F)^*$ (for both spin directions) by using the relation

$$\chi_m = \mu_B^2 N(\varepsilon_F)^* . \tag{5}$$

The densities of states $N(\varepsilon_F)^*$ are estimated to be 0.95 states/eV atom for $CuRh_2S_4$ and 0.72 states/eV atom for $CuRh_2Se_4$. These values of $N(\varepsilon_F)^*$ are about two times smaller than those estimated from the γ values of the specific heat, which will be described below.

D. Specific heats

The temperature dependences of the specific heats of $CuRh_2S_4$ and $CuRh_2Se_4$ are shown in Figs. 11 and 12. Superconducting transitions take place at 4.64 and 3.37 K, respectively. It is noted that, unfortunately, some experimental errors are included in the result for $CuRh_2Se_4$ just above T_c. Specific-heat results for these two samples are also displayed as C/T vs T^2. The dashed lines represent the extrapolations from the normal-state specific heats to $T=0$ K. The C/T vs T^2 plots yield fairly straight lines at low temperature. Here, the undulation around $T \sim 5$ K for $CuRh_2Se_4$ in Fig. 12 comes from the experimental errors. The specific heats are well fitted by

$$C = \gamma T + \beta T^3 . \tag{6}$$

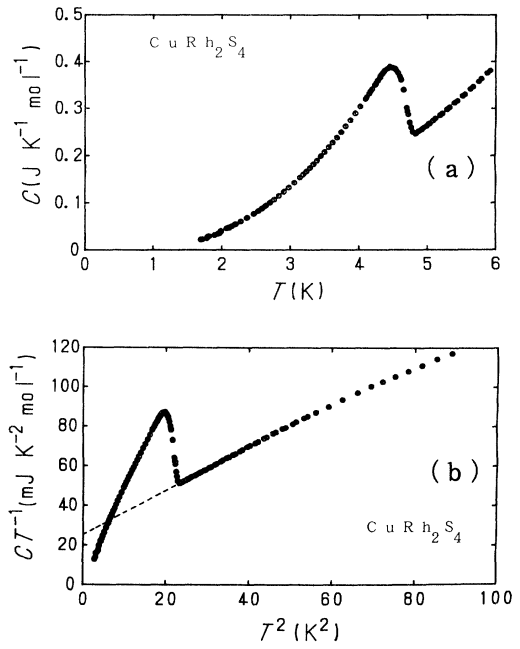

FIG. 11. (a) Specific heat of $CuRh_2S_4$ as a function of temperature. (b) The plot of C/T vs T^2.

The values of γ are extracted from the $T=0$ K intercept of the extrapolated lines. The magnitudes of γ are rather large, and give high densities of states at the Fermi surface.

From the value of β, we estimate the Debye temperature Θ by using the relation

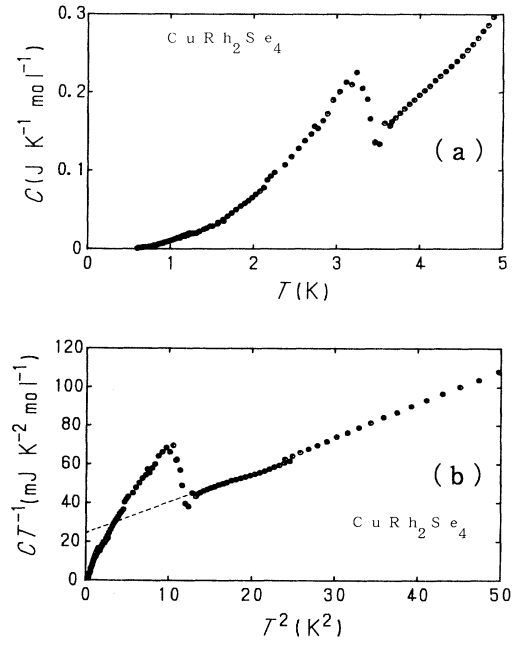

FIG. 12. (a) Specific heat of $CuRh_2Se_4$ as a function of temperature. (b) The plot of C/T vs T^2.

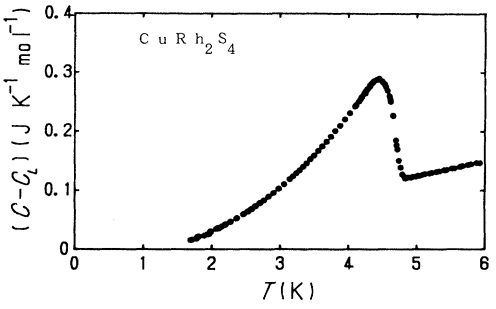

FIG. 13. Electronic specific heat $(C-C_L)$ of $CuRh_2S_4$ as a function of the temperature after subtracting the lattice specific-heat contribution C_L.

$$\beta=\frac{12\pi^4 r N_0 k_B}{5\Theta^3}\ , \tag{7}$$

with r being the number of atoms per formula unit ($r=7$ for these materials), N_0 Avogadro's number, and k_B Boltzmann's constant. Equation (7) yields $\Theta=230$ and 211 K for $CuRh_2S_4$ and $CuRh_2Se_4$, respectively. The Debye temperatures of these compounds are rather small in comparison with the value of Θ for an oxide spinel compound such as $LiTi_2O_4$.[26,27] $LiTi_2O_4$ has $\beta=0.043$ mJ/K^4 mol f.u., giving $\Theta=685$ K.

The origin of this lower value of the Debye temperature in these compounds might be attributed to a rattling of the cations within a correspondingly large space between the sulfur anions.[28] In sulfides such as CuV_2S_4,[29] $CuRh_2S_4$, and $CuRh_2Se_4$, the cations have a large space for moving in the sulfur anion network. Consequently, lattice vibrations can easily be excited in the crystal. The difference in the Debye temperature between the oxides and sulfides could come from this enhanced excitation of the cations in the sulfides. The magnitude of T_c increases in proportion to the Debye temperature on the basis of the BCS theory.

Figures 13 and 14 display the electronic specific heats after subtracting the lattice contributions C_L. The measurement was not extended below 1.6 K for $CuRh_2S_4$ in Fig. 13. The small dots represent the extrapolated values from higher temperatures.

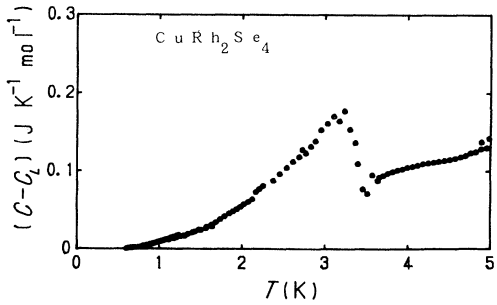

FIG. 14. Electronic specific heat $(C-C_L)$ of $CuRh_2Se_4$ as a function of the temperature after subtracting the lattice specific-heat contribution C_L.

E. Entropy and energy gap

Entropies $S(T)=\int_0^T[(C-C_L)/T]dT$ are obtained by measuring the area under the curve of $(C-C_L)/T$ vs T for $CuRh_2S_4$ and $CuRh_2Se_4$ in the normal and superconducting states as functions of temperature. The entropies decrease markedly on cooling below the superconducting transition temperatures.

The specific heat has the form

$$C=C_L+C_{es} , \tag{8}$$

where C_L is the lattice contribution and is assumed to be identical to $C_L(=\beta T^3)$. The electronic parts, C_{es}, of the specific heats in the superconducting state is plotted on a log scale vs T_c/T in Figs. 15 and 16. The electronic contribution C_{es} may be approximated according to the BCS theory,[30] for $T<0.5T_c$, by

$$C_{es}=(a\gamma T_c)\exp[-bT_c/T] , \tag{9}$$

where a and b are constants. They are listed in Table I.

We extract a value for the electron-phonon interaction parameter λ_{ep} from the Coulomb repulsion parameter μ^* and the experimentally determined transition temperature T_c and the Debye temperature Θ:[31]

$$\lambda_{ep}=\frac{1.04+\mu^*\ln(\Theta/1.45T_c)}{(1-0.62\mu^*)\ln(\Theta/1.45T_c)-1.04} . \tag{10}$$

Here we assume empirically $\mu^*=0.13$,[31] since T_c is less sensitive to μ^* than to λ_{ep}. Using Eq. (9), we obtain $\lambda_{ep}=0.683$ ($CuRh_2S_4$) and $\lambda_{ep}=0.635$ ($CuRh_2Se_4$). These results indicate that these two compounds can be classified as intermediate-coupled superconductors.

The enhancement of γ by the electron-phonon interaction is given by the relation[31]

$$\gamma=\tfrac{1}{3}k_B^2\pi^2N(\varepsilon_F)^* =\tfrac{1}{3}k_B^2\pi^2N(\varepsilon_F)(1+\lambda_{ep}) , \tag{11}$$

where $N(\varepsilon_F)$ is the band-structure density of states at the Fermi level (for both spin directions). The value of $N(\varepsilon_F)$ is found to be $N(\varepsilon_F)=0.901$ states/eV atom for $CuRh_2S_4$ and 0.964 states/eV atom for $CuRh_2Se_4$. The values of $N(\varepsilon_F)^*$ are 1.52 and 1.58 states/eV atom for $CuRh_2S_4$ and $CuRh_2Se_4$, respectively. These values of $N(\varepsilon_F)^*$ are larger than those from the Pauli susceptibilities obtained from Eq. (5).

The specific-heat jump ΔC from the normal to the superconducting states at T_c gives the normalized value $\Delta C/(\gamma T_c)$. These values of the two compounds are listed in Table I. The value of $\Delta C/(\gamma T_c)$ for $CuRh_2S_4$ is considerably larger than the BCS prediction of 1.43, and the value is slightly smaller than the BCS prediction for $CuRh_2Se_4$. These facts suggest that these compounds are not simple weak-coupled superconductors but are intermediate-coupled superconductors.

The thermodynamic critical field $H_c(T)$ can be determined by the relationship[32,33]

$$G_N(T)-G_S(T)=\int_T^{T_c}[S_N(T)-S_S(T)]dT =[V_m/8\pi][H_c(T)]^2 . \tag{12}$$

Using the value of the entropy difference, Eq. (12) was integrated graphically and the $H_c(T)$ values were obtained by using the molar volume V_m given in Table I. The critical fields at $T=0$ K are found to be 704 Oe in $CuRh_2S_4$ and 445 Oe in $CuRh_2Se_4$.

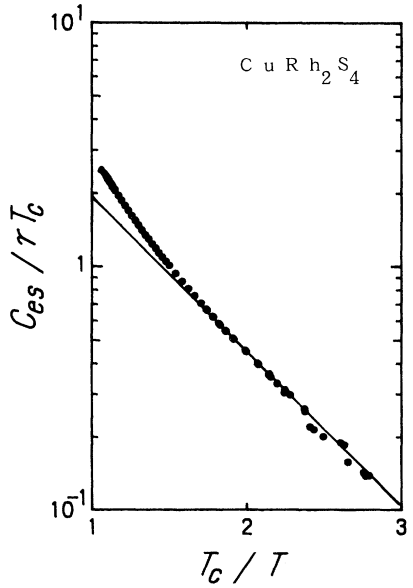

FIG. 15. Reduced superconducting electronic specific heat $C_{es}/\gamma T_c\equiv(C-C_L)/\gamma T_c$ of $CuRh_2S_4$ on a log scale vs T_c/T. The logarithms are to base 10.

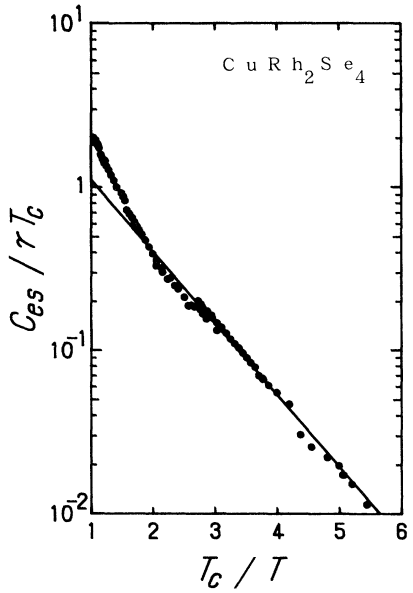

FIG. 16. Reduced superconducting electronic specific heat $C_{es}/\gamma T_c\equiv(C-C_L)/\gamma T_c$ of $CuRh_2Se_4$ on a log scale vs T_c/T. The logarithms are to base 10.

TABLE I. Superconducting and normal-state properties for $CuRh_2S_4$ and $CuRh_2Se_4$. The u parameter denotes anion positions; see Ref. 6. Values of Seebeck coefficient at 300 K are cited from Ref. 3.

Property	Units	$CuRh_2S_4$	$CuRh_2Se_4$
Lattice const. a	Å	9.787	10.269
u parameter		0.384	0.384
V_m	cm^3/mol	70.58	81.54
T_c	K	4.70	3.48
γ	mJ/K^2 mol f.u.	25	26
Θ	K	230	211
$N(\varepsilon_F)$ (from γ)	states/eV atom	0.90	0.96
λ_{ep}		0.68	0.64
χ_0	10^{-4} emu/mol f.u.	3.4	3.2
S (Seebeck)	μV/K	+25	+7.3
$\Delta C/(\gamma T_c)$		1.82	1.31
$H_{c2}(0)$	kOe	20.0	4.40
$C_{es}=(a\gamma T_c)\exp[-bT_c/T]$ $(T<0.5T_c)$		$a=8.73$ $b=1.50$	$a=3.00$ $b=1.02$
$H_c(0)$ (from free energy)	Oe	704	445
$H_c(0)=[\gamma T_c^2/(0.170V_m)]^{1/2}$	Oe	680	470
$2\Delta(0)/k_BT_c=\frac{4\pi}{\sqrt{3}}\left[\frac{H_c(0)^2V_m}{8\pi\gamma T_c^2}\right]^{1/2}$		3.51	3.51
$\xi_{GL}(0)$	Å	128	274
$\lambda(0)$	Å	2670	1810
$\kappa(0)=\lambda/\xi_{GL}$		21	6.6
$H_{c1}(0)=\frac{\phi_0\ln\kappa}{4\pi\lambda^2}$	Oe	70	95

On the other hand, the BCS theory predicts the magnitude of $H_c(0)$ by the relation

$$H_c(0)=[\gamma T_c^2/(0.170V_m)]^{1/2} . \quad (13)$$

Taking the experimental values for both compounds into consideration Eq. (13) gives 680 Oe for $CuRh_2S_4$ and 470 Oe for $CuRh_2Se_4$, which are close to the values from Eq. (12).

According to Goodman,[34] the value of the energy gap at $T=0$ can be obtained from the relation

$$\frac{2\Delta(0)}{k_BT_c}=\frac{4\pi}{\sqrt{3}}\left[\frac{H_c(0)^2V_m}{8\pi\gamma T_c^2}\right]^{1/2} . \quad (14)$$

Values of $2\Delta(0)/k_BT_c$ are calculated by using this relation and are found to be 3.511 in $CuRh_2S_4$ and 3.512 in $CuRh_2Se_4$, which are in very good agreement with the BCS prediction of 3.53.

F. Upper critical field H_{c2}

Figure 17 shows the magnetization as a function of magnetic field at 4.5 K for $CuRh_2S_4$, which is not far below the transition temperature ($T_c=4.70$ K). The initial magnetization curve for $CuRh_2Se_4$ at 2.0 K is given in Fig. 18. The upper critical field H_{c2} can be extracted from the magnetization curve. The temperature dependence of H_{c2} is plotted in Fig. 19. Unfortunately, we have only obtained H_{c2} up to 10 kOe and 2.0 K because of instrumental limitations. In Fig. 19(b), the temperature dependence of the thermodynamic critical fields $H_c(T)$ is also shown.

According to the theory of type-II superconductors, the upper critical field at $T=0$ can be estimated from the relation[35–38]

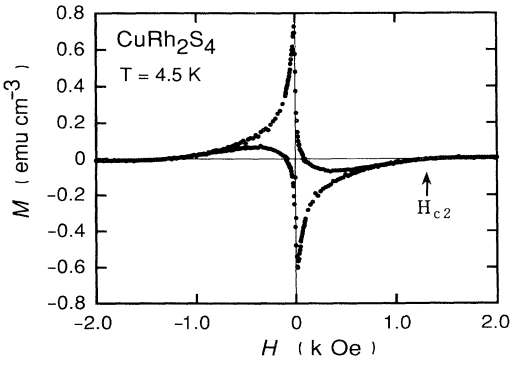

FIG. 17. Magnetization as a function of magnetic field at 4.5 K for $CuRh_2S_4$. $H_{c2}=1.30$ kOe is marked by the arrow.

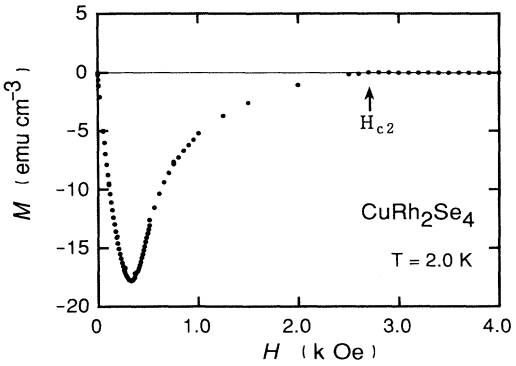

FIG. 18. Magnetization as a function of magnetic field at 2.0 K for $CuRh_2Se_4$; only the first increasing curve is presented. $H_{c2}=2.70$ kOe is marked by the arrow.

$$H_{c2}(0)=0.693T_c(-dH_{c2}/dT)_{T_c}\ , \tag{15}$$

assuming the dirty limit. Using this Eq. (15) the values of H_{c2} are found to be 20.0 and 4.40 kOe for $CuRh_2S_4$ and $CuRh_2Se_4$, respectively. These values of H_{c2} are slightly smaller than those found by former workers,[8] where simple extrapolated values have been reported. The Ginzburg-Landau (GL) coherence length ξ_{GL} can be estimated to be $\xi_{GL}=128$ Å in $CuRh_2S_4$ and 274 Å in $CuRh_2Se_4$ at $T=0$ K from the relation[39]

$$H_{c2}=\frac{\phi_0}{2\pi\xi_{GL}^2}\ , \tag{16}$$

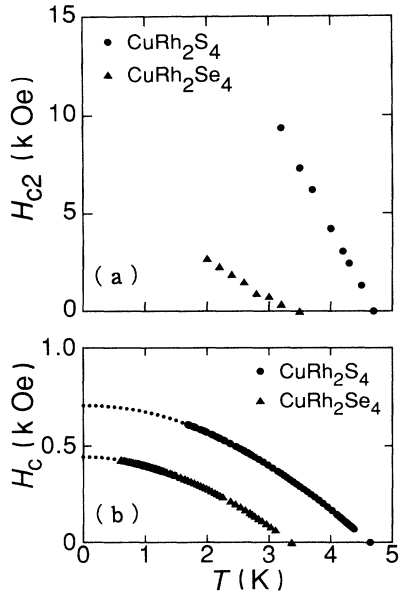

FIG. 19. (a) Upper critical fields H_{c2} as functions of temperature for $CuRh_2S_4$ and $CuRh_2Se_4$. (b) The thermodynamic critical fields H_c vs temperature. Here, small dots in H_c are extrapolated values.

where $\phi_0=ch/2e=2.07\times10^{-7}$ G cm^2 is the quantum of flux. This is the highest field at which superconductivity can nucleate in the interior of bulk samples. The penetration depth λ can be determined from the relation

$$H(0)=\frac{\phi_0}{2\sqrt{2}\pi\lambda\xi_{GL}}\ . \tag{17}$$

The penetration depths λ at $T=0$ K calculated from Eq. (17) are 2670 Å in $CuRh_2S_4$ and 1810 Å in $CuRh_2Se_4$, respectively. The Ginzburg-Landau parameters $\kappa=\lambda/\xi_{GL}$ are found to be $\kappa=21$ in $CuRh_2S_4$ and 6.6 in $CuRh_2Se_4$. This indicates that both compounds are typical type-II superconductors.

The lower critical field at which magnetic flux first penetrates can be expressed as

$$H_{c1}=\frac{\phi_0\ln\kappa}{4\pi\lambda^2}\ . \tag{18}$$

Estimated values are $H_{c1}=70$ Oe in $CuRh_2S_4$ and 95 Oe in $CuRh_2Se_4$. It is difficult to measure the values of H_{c1} accurately from the low-temperature magnetization curves.

G. Deviation function of thermodynamic critical field

The deviations of the reduced thermodynamic critical field $H_c(t)/H_c(0)$ from the parabola $1-t^2$ are examined in order to check "coupling strength" (here t is the reduced temperature T/T_c). Figure 20 shows the analyzed results for $CuRh_2S_4$ and $CuRh_2Se_4$ with the theoretical value of $2\Delta(0)/k_BT_c=3.90$, which was obtained by assuming $\Delta(T)/\Delta^{BCS}(T)=$const. The only adjustable parameter in the model is this constant value, which provides a means of "scaling" the BCS gap.[40,41] These results suggest that neither $CuRh_2S_4$ nor $CuRh_2Se_4$ is a strong-coupling superconductor but indicate that they are locat-

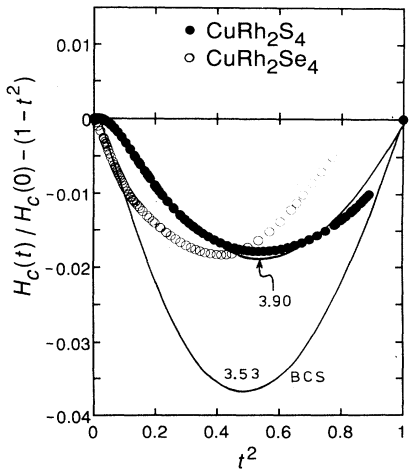

FIG. 20. Deviation function of reduced thermodynamic critical field $D(t)=H_c(t)/H_c(0)-(1-t^2)$, for $CuRh_2S_4$ and $CuRh_2Se_4$, where $t=T/T_c$. The solid curves are the results for the energy gap values of 3.53 (BCS) and 3.90; see (Ref. 40).

ed between weak- and intermediate-coupling superconductors.

H. Coherence peak of $1/T_1$ for Cu NMR in $CuRh_2S_4$

The measured values of the nuclear spin-lattice relaxation time T_1 of copper nuclei in $CuRh_2S_4$ as a function of inverse temperature are shown in Fig. 21. The plot of $1/T_1$ as a function of temperature is also shown in Fig. 22. The transition temperature T_c is reduced in the presence of the applied magnetic field of 11 kOe.

In the energy gap there are no available states at all, and the missing states are piled up on either side. At temperatures just below T_c, the energy gap is still very narrow and $<k_BT$, so that the piled-up states on either side result in an appreciable increase of relaxation rate $1/T_1$ over that in the normal state. Then T_1 decreases rapidly just below T_c and then rapidly increases again further below T_c. As can be seen in Fig. 22, we clearly find an enhancement effect in $1/T_1$. At lower temperatures, the gap becomes wider than k_BT, and the relaxation rate $1/T_1$ eventually exponentially approaches zero. The energy gap can also be estimated from this temperature dependence. The best fit of the data gives $2\Delta(0)/k_BT_c=3.60$. This result is in reasonable agreement with the value obtained from Eq. (14) using the specific-heat results.[42–44]

Below 100 K, in the normal state, the temperature dependence of $1/T_1$ follows a Korringa law with $T_1T=0.44$ s K. The value of the Knight shift has a weak temperature dependence. The magnitude of the Knight shift at Cu nuclei, which is extrapolated to $T=0$ K, is estimated to be -0.088% due to the d-wave spin-polarization effect in Cu atoms. These results confirm $CuRh_2S_4$ to be a simple Pauli paramagnet without appreciable electron-electron correlation.[14]

I. Comparison with some other normal-spinel compounds

The magnetic properties of $CuRh_2O_4$ can be adequately discussed on the basis of the ionic point of view. The valence of copper is Cu^{2+} and the rhodium Rh^{3+} is nonmagnetic with a low-spin state in the filled t_{2g} level. The

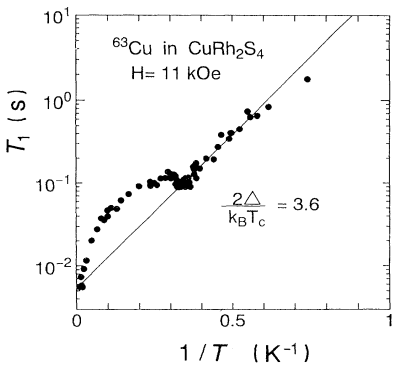

FIG. 21. Copper nuclear spin-lattice relaxation time T_1 in $CuRh_2S_4$ as a function of inverse temperature.

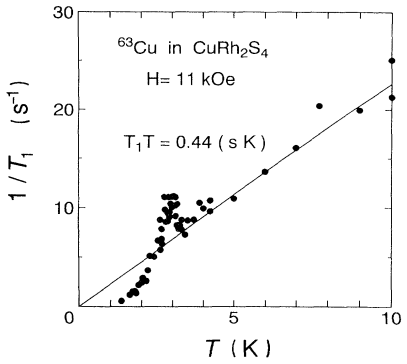

FIG. 22. Inverse copper nuclear spin-lattice relaxation time T_1 in $CuRh_2S_4$ as a function of temperature; these are just the same experimental results shown in Fig. 21.

Néel temperature of $CuRh_2O_4$ is 24.0 K, below which the magnetic moments due to localized-spin Cu^{2+} ($s=\frac{1}{2}$) become ordered.[45] $CuCo_2S_4$ does not show superconductivity but stays metallic down to 0.05 K.[4]

Recently, a temperature-induced metal-insulator transition has been observed in $CuIr_2S_4$ at 230 K.[21–24] At around 230 K, $CuIr_2S_4$ exhibits a structural phase transition from a low-temperature tetragonal phase (insulating) to a high-temperature cubic phase (metallic). There is no localized magnetic moment in either the insulating or metallic phase. On the other hand, $CuIr_2Se_4$ stays metallic down to 0.5 K without any phase transition.[23]

The conducting and magnetic properties of $CuRh_2S_4$ and $CuRh_2Se_4$ have been explained using models for the electronic structure of thiospinels given by Lotgering and Van Stapele[3] and Goodenough.[1] The p-type metallic conduction is attributed to hole conduction in the valence band. The observation of a small and temperature-independent susceptibility can be explained by the absence of magnetic ions. Lotgering and co-workers[2,3,46] suggested that the valencies can be represented by the formula $Cu^{+}Rh_2^{3+}S_3^{2-}S^{-}$ where S^{-} denotes a hole in the valence band. The lack of a cooperative Jahn-Teller distortion has been explained by the presence of Cu^{+} instead of Cu^{2+} on the A sites.[2,3]

An alternative model presented by Goodenough[1,47] assumed an ionic $Cu^{2+}Rh_2^{3+}S_4^{2-}$ with a delocalization of the T_{2g} orbitals of Cu^{2+} caused by the formation of a partially filled σ^* band. For the thiospinels, cation-anion covalence can occur with both octahedral and tetrahedral ions. Because the sulfide ions have four nearest-neighbor cations, σ bonding is much stronger than π bonding and the partially filled band is composed of antibonding σ^* states. It appears that the metallic conductivity in the thiospinels may be due to partially filled band states. If molecular orbitals are formed between the metal ions and the anions, the T_{2g} levels of the Cu^{2+} ions are no longer localized. Since these levels are responsible for any distortion produced at the Cu^{2+} on tetrahedral sites, delocalizing them would remove the driving force for the distortion.

Although our studies in this paper have focused on the

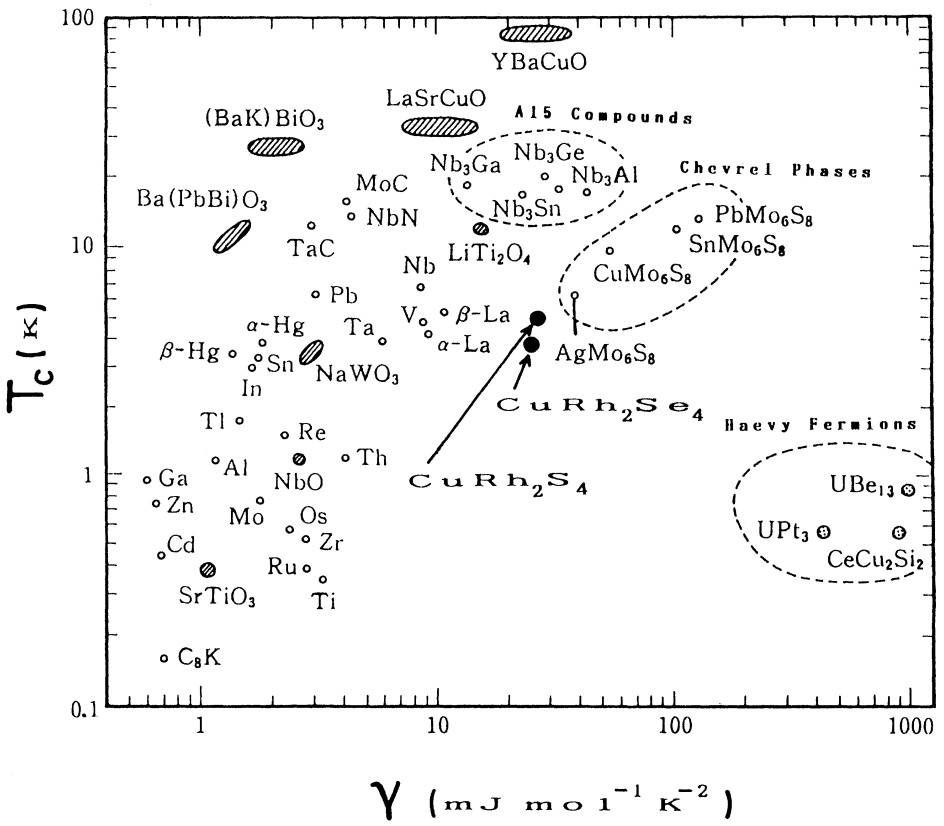

FIG. 23. Superconducting transition temperature vs the electronic specific-heat constant γ for various superconductors (T_c vs γ plot). Two black circles indicate the locations of $CuRh_2S_4$ and $CuRh_2Se_4$.

characteristics of the superconductivity, it is our hope that our measurements presented here will also lead to fruitful discussion on the electronic structure of these compounds.

IV. SUMMARY

In the normal state, this work gives $\rho(300\ \text{K})=8.0\times10^{-3}\ \Omega\,\text{cm}$, $\gamma=25$ mJ/mol K^2, and $\Theta=230$ K for $CuRh_2S_4$, and $\rho(300\ \text{K})=4.6\times10^{-4}\ \Omega\,\text{cm}$, $\gamma=26$ mJ/mol K^2, and $\Theta=211$ K for $CuRh_2Se_4$. In the superconducting state, our experimental study has shown that these spinel compounds are type-II superconductors with GL parameters of $\kappa=21$ ($CuRh_2S_4$) and 6.6 ($CuRh_2Se_4$). For both compounds, the value of the gap ratio $2\Delta(0)/k_BT_c$ gives values between 3.1 and 3.9 for various measurements. The copper nuclear spin-lattice relaxation rate exhibits distinctly a coherence peak. These spinel compounds are not strong-coupling superconductors but are located between weak- and intermediate-coupling superconductors. The lower T_c of both these rhodium spinels, as compared to $LiTi_2O_4$, is probably due to the lower Debye temperatures Θ we observe. The superconducting transition temperature T_c vs the electronic specific-heat constant γ is plotted for various specimens in Fig. 23. The solid circles indicate $CuRh_2S_4$ and $CuRh_2Se_4$. This figure indicates that these sulfo- and selenospinels are most closest related to the molybdenum sulfide chevrel-phase materials.

ACKNOWLEDGMENTS

The authors would like to thank Professor Hidehiko Ishimoto and Professor Nobuo Môri, the Institute for Solid State Physics, the University of Tokyo, for use of the facilities, and for warm encouragement. The authors wish to thank Professor P. C. Canfield (Iowa State University) for his helpful comments and critical reading of this manuscript. The present work was supported by a Grant-in-Aid for Special Project Research (No. 06216206) from the Ministry of Education, Science and Culture of Japan.

*Author to whom all correspondence should be addressed.

[1]J. B. Goodenough, J. Phys. Chem. Solids **30**, 261 (1969).
[2]F. K. Lotgering and R. P. Van Stapele, Solid State Commun. **5**, 143 (1967).
[3]F. K. Lotgering and R. P. Van Stapele, J. Appl. Phys. **39**, 417 (1968); F. K. Lotgering, J. Phys. Chem. Solids **30**, 1429 (1969); F. J. DiSalvo and J. V. Waszczak, Phys. Rev. B **26**, 2501 (1982).
[4]N. H. Van Maaren, G. M. Schaeffer, and F. K. Lotgering, Phys. Lett. **25A**, 238 (1967).

[5]M. Robbins, R. H. Willens, and R. C. Miller, Solid State Commun. **5**, 933 (1967).
[6]P. P. Dawes and N. W. Grimes, Solid State Commun. **16**, 139 (1975).
[7]R. N. Shelton, D. C. Johnston, and H. Adrian, Solid State Commun. **20**, 1077 (1976).
[8]G. M. Schaeffer and M. H. Van Maaren, in *Proceedings of the 11th International Conference on Low Temperature Physics,* edited by J. F. Allen (University of St. Andrews Press, St. Andrews, Scotland, 1969), Vol. 2, p. 1033.
[9]M. H. Van Maaren, H. B. Harland, and E. E. Havinga, Solid State Commun. **8**, 1933 (1970).
[10]T. Bitoh, T. Hagino, Y. Seki, S. Chikazawa, and S. Nagata, J. Phys. Soc. Jpn. **61**, 3011 (1992).
[11]T. Shirane, T. Hagino, Y. Seki, T. Bitoh, S. Chikazawa, and S. Nagata, J. Phys. Soc. Jpn. **62**, 374 (1993).
[12]K. Kumagai, M. Abe, S. Tanaka, Y. Maeno, T. Fujita, and K. Kadowaki, Physica B **165&166**, 1297 (1990).
[13]K. Kumagai and Y. Nakamura, Physica C **157**, 307 (1989).
[14]K. Kumagai *et al.* (unpublished).
[15]Y. Aoki, T. Suzuki, T. Fujita, T. Takabatake, S. Miyata, and H. Fujii, J. Phys. Soc. Jpn. **61**, 684 (1992).
[16]A. H. Wilson, *The Theory of Metals,* 2nd ed. (Cambridge University Press, Cambridge, England, 1956).
[17]G. W. Webb, Z. Fisk, J. J. Engelhardt, and S. D. Bader, Phys. Rev. B **15**, 2624 (1977); D. W. Woodard and G. D. Cody, Phys. Rev. **136**, A166 (1964).
[18]A. H. Wilson, Proc. R. Soc. London **167**, 580 (1938); N. F. Mott, *ibid.* **153**, 699 (1936).
[19]M. Sato and Y. Ishii, J. Appl. Phys. **66**, 983 (1989).
[20]S. Gregory, Phys. Rev. Lett. **40**, 723 (1978).
[21]S. Nagata, T. Hagino, Y. Seki, and T. Bitoh, Physica B **194-196**, 1077 (1994).
[22]T. Furubayashi, T. Matsumoto, T. Hagino, and S. Nagata, J. Phys. Soc. Jpn. **63**, 3333 (1994).
[23]T. Hagino, Y. Seki, and S. Nagata, in *Proceedings of the International Conference on Materials and Mechanisms of Superconductivity High Temperature Superconductors (M^2S-HTSC) IV, Grenoble, France, 1994,* edited by P. Wyder [Physica C **235-240**, 1303 (1994)].
[24]T. Hagino, T. Tojo, T. Atake, and S. Nagata, Philos. Mag. B (to be published).
[25]*Magnetic Properties of Coordination and Organometallic Transition Metal Compounds,* edited by K.-H. Hellwege and O. Madelung, Landolt-Börnstein, New Series, Vol. 8 (Springer-Verlag, Berlin, 1976), p. 27.
[26]D. C. Johnston, J. Low Temp. Phys. **25**, 145 (1976).
[27]R. W. McCallum, D. C. Johnston, C. A. Luengo, and M. B. Maple, J. Low Temp. Phys. **25**, 177 (1976).
[28]R. D. Shannon, J. Appl. Phys. **73**, 348 (1993).
[29]T. Hagino, Y. Seki, S. Takayanagi, N. Wada, and S. Nagata, Phys. Rev. B **49**, 6822 (1994).
[30]J. Bardeen, L. N. Cooper, and J. R. Schrieffer, Phys. Rev. **108**, 1175 (1957).
[31]W. L. McMillan, Phys. Rev. **167**, 331 (1968).
[32]E. S. R. Gopal, *Specific Heats at Low Temperatures* (Plenum, New York, 1966), p. 74.
[33]P. H. Pan, D. K. Finnemore, A. J. Bevolo, H. R. Shanks, B. J. Beaudry, F. A. Schmidt, and G. C. Danielson, Phys. Rev. B **21**, 2809 (1980).
[34]B. B. Goodman, C. R. Acad. Sci. **246**, 3031 (1958).
[35]R. R. Hake, Appl. Phys. Lett. **10**, 189 (1967).
[36]R. R. Hake, Phys. Rev. **158**, 356 (1967).
[37]T. P. Orlando, E. J. McNiff, Jr., S. Foner, and M. R. Beasley, Phys. Rev. B **19**, 4545 (1979).
[38]N. R. Werthamer, E. Helfand, and P. C. Hohenberg, Phys. Rev. **147**, 295 (1966).
[39]For example, M. Tinkham, *Introduction to Superconductivity* (McGraw-Hill, New York, 1975), p. 129.
[40]H. Padamsee, J. E. Neighbor, and C. A. Shiffman, J. Low Temp. Phys. **12**, 387 (1973), and references therein.
[41]D. K. Finnemore and D. E. Mapother, Phys. Rev. **140**, A507 (1965).
[42]A. G. Redfield, Phys. Rev. Lett. **3**, 85 (1959).
[43]Y. Masuda and A. G. Redfield, Phys. Rev. **125**, 159 (1962).
[44]Y. Masuda, Phys. Rev. **126**, 1271 (1962).
[45]G. Blasse, Philips Res. Rep. **18**, 383 (1963); S. Nagata *et al.* (unpublished).
[46]F. K. Lotgering, J. Phys. Chem. Solids **30**, 1429 (1969).
[47]J. B. Goodenough, Solid State Commun. **5**, 577 (1967).